Armenian Journal of Physics, 2018, vol. 11, issue 2, pp. 84-90

Impedance characteristics of p-Si /$Ba_xSr_{1-x}TiO_3$ heterojunction prepared by pulsed laser deposition method

V. Buniatyan, A. Davtyan, V. Begoyan, H. Dashtoyan

National Polytechnic University of Armenia (NPUA), Yerevan

Received 09 June 2018

Abstract. $p-Si\,/\,Ba_xSr_{1-x}TiO_3$ heterojunction properties are investigated by electrochemical impedance spectroscopy method for the first time. The general equivalent circuit model is proposed in circuit description code as: C_f, R_f, C_h,R_h,R_P, where C_f, R_f are the $Ba_xSr_{1-x}TiO_3$ film conditioned capacitance and resistance, C_h, R_h are the heterojunction depletion layer capacitance and resistance, respectively, R_P is the series resistance. It is stated that the Bode plot curves of the structure in air mostly affected by the depletion layer capacitance of heterojunction $C_h(V)$.

Keywords: ferroelectric, heterojunction, impedance spectroscopy

1. Introduction

In the past few decades impedance spectroscopy (IS) has become firmly established as a primary method of evaluating electrochemical, bio-chemical as well as electro-physical processes in structures [1,2]. This technique has grown tremendously in stature over the past few years and is now being widely employed in a wide variety of scientific fields. Often, IS reveals information about the reaction mechanism (in solutions and in solids) of electrochemical processes, where different reaction steps can be dominate at certain frequencies, and the frequency response shown by IS can help identify the rate limiting step [1].

The impedance spectrum reflects absorption/desorption, oxidation-reduction reactions as well as mass migration across in the electrochemical cells and electrodes [1,2], which are determined by the electrical, elecrto-physical, physio-chemical properties of the medium and the electrode materials. In IS measurement, a sinusoidal (ac) voltage is applied at varying frequencies to an electrode system under test. The response is analyzed in terms of resultant current amplitude and phase. The current signal can be analyzed as a sum of sinusoidal functions (Fourier series). Electrochemical impedance is normally measured using a small excitation signal to be sure that the structure’s response is pseudo-linear. In a linear (pseudo-linear) system the current response to a sinusoidal potential will be sinusoidal at the same frequency but shifted in phase. Over a frequency bandwidth of interest, the impedance spectrum can be presented in various ways known as "Nyquist plot" and “Bode plot” [1,2].

Integrating the perovskite-type transition metal oxides with the silicon technology would introduce the possibility for multifunctional microelectronic device such as field-effect transistors [3], nonvolatile ferroelectric random access memory (FRAM) [4], surface acoustic wave resonators and tunable varactors [5], chemical and bio-sensors [6,7], transducers and actuators (including ultrasonic, infrared and imaginary applications) [8-11], microelectro-mechanical systems (MEMS) [12].

Moreover, during last decade, increasing attention was attributed to heterojunctions based on ferroelectric and multiferroic films grown on semiconductors [13-19]. These devices are a novel class of solid-state devices and are expected to be very promising for wide applications in above-mentioned fields.

In this context, the aim of the presented paper is to investigate the behavior of $p-Si/Ba_xSr_{1-x}TiO_3$ semiconductor heterojunction system by means of IS method with the aim to utilize it in above-mentioned field for the future.

2. Experimental

For the fabrication of $p-Si/Ba_xSr_{1-x}TiO_3$ heterojunction structures on the $p-Si$ wafer (<100>, boron doped, $\rho = 1-10\Omega cm$, thickness: $350\mu m$), the $Ba_{0.25}Sr_{0.75}TiO_3$ films ($\sim 100nm$ thick) were prepared by pulsed laser deposition (PLD) technique using targets fabricated by the self-propagating high-temperature synthesis (SHS) method [7,20].

The main advantages of the PLD technique are the compatibility with silicon technology, the short deposition time, the possibility of deposition of insulators, as well as multi-component materials [6,7]. The deposition was performed in an oxygen atmosphere (gas flow $30ml/\min$, pressure $2\times10^{-3}mbar$) using a KrF-excimer laser (wavelength $248nm$, pulse length $20ns$, pulse frequency $10Hz$ and an energy density of $2.5J/cm^2$) [7,20]. As contact layer, a $300nm$ *Al* layer was deposited on the backside of the top p-Si substrate. The processed wafer was diced into separate chips (chip size: $10\times10mm^2$). The prepared structures have been characterized in air by means of IS (Bode plot) method. For the experiments in air, the structures were mounted into a homemade measuring cell and contacted on their front size by Ag past point contact (area approximately between $0.042cm^2$ and $0.071cm^2$, Fig.1). The IS measurements were carried out by applied polarization voltages of $(-3V),(-0.7V),(+3V)$ to obtain different regimes of operation of heterojunction structures and impedance spectra were recorded with an impedance analyzer module (Zennium, ZahnerElektrik GmbH, Germany) covering a frequency range from 1Hz to 1MHz. All potential values are referred to the Ag point contact. For the details of the experimental setup, see [6,7,20]. In Fig.2, the Bode plot of $Al-p-Si-Ba_{0.25}Sr_{0.75}TiO_3-Ag$ structure for the different bias voltage is presented. As it follows from Fig.2, in air the structure exhibits approximately pure capacitive character for different bias voltages.

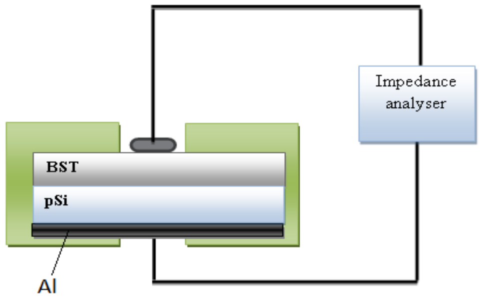

Fig. 1.Schematic representation of the experimental set-up used for IS

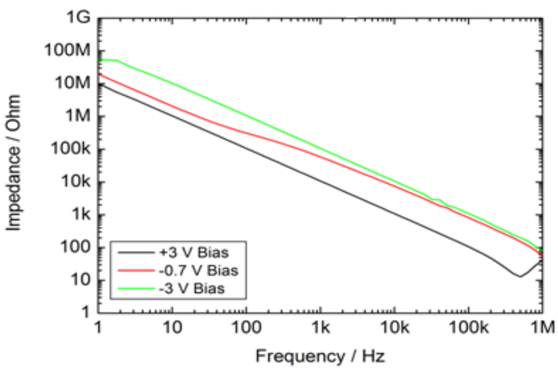

Fig.2. Bode plot of an Al−pSi− $Ba_{0.25}Sr_{0.75}TiO_3$− Ag structure for different bias voltages

The schematic cross-section and energy band diagram of the heterojunction structure is shown in Fig.3. In Fig.3.*b* E_W is the vacuum level, $\Delta E_c, \Delta E_V$ are the conductance and valence band offsets, respectively: $\Delta E_c = E_{C2} - E_{C1} - q\Phi_{B0}$ or $\Delta E_c = (\chi_1 - \chi_2) \approx -0.15\,eV$, $q\Phi_{B0}$ is the heterojunction built in potential, $q\Phi_{B0} = \varphi_1(x) + \varphi_2(x) \cong 0.61\,eV, \Delta E_V = (\chi_1 - \chi_2) + (E_{gBST} - E_{gSi}) \approx 1.95$ eV, $\chi_1(\chi_1 \approx 3.9)$eV, $\chi_2(\chi_2 \approx 4.05)$eV, are the electron affinities of BST and Si, respectively, F_{nF1} and F_{nF2} are the Fermi-quasi level for electrons, E_{if} and E_{i2} are the intrinsic Fermi level in BST and Si, respectively, W_1 and W_2 are the space-charge depletion layer widths in BST and Si, respectively, N_A is the concentration of acceptors in $p-Si$.

The energy band diagram has been structured taking into account that: a) in the heterojunction surface in contact to crystalline $p-Si$ due to an inevitable presented high oxygen vacancies concentration "endows" ferroelectric n-type semiconductor properties; b) oxygen vacancies create donor-like electron deep-trap levels (N_t) with the characteristic energies E_t in the band gap of ferroelectrics; c) the dielectric permittivity of ferroelectric films is non-linear dependent on the electric field.

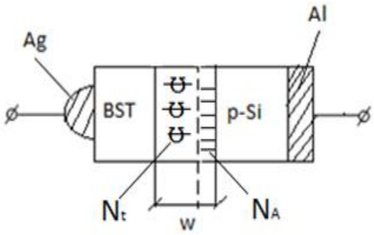

a

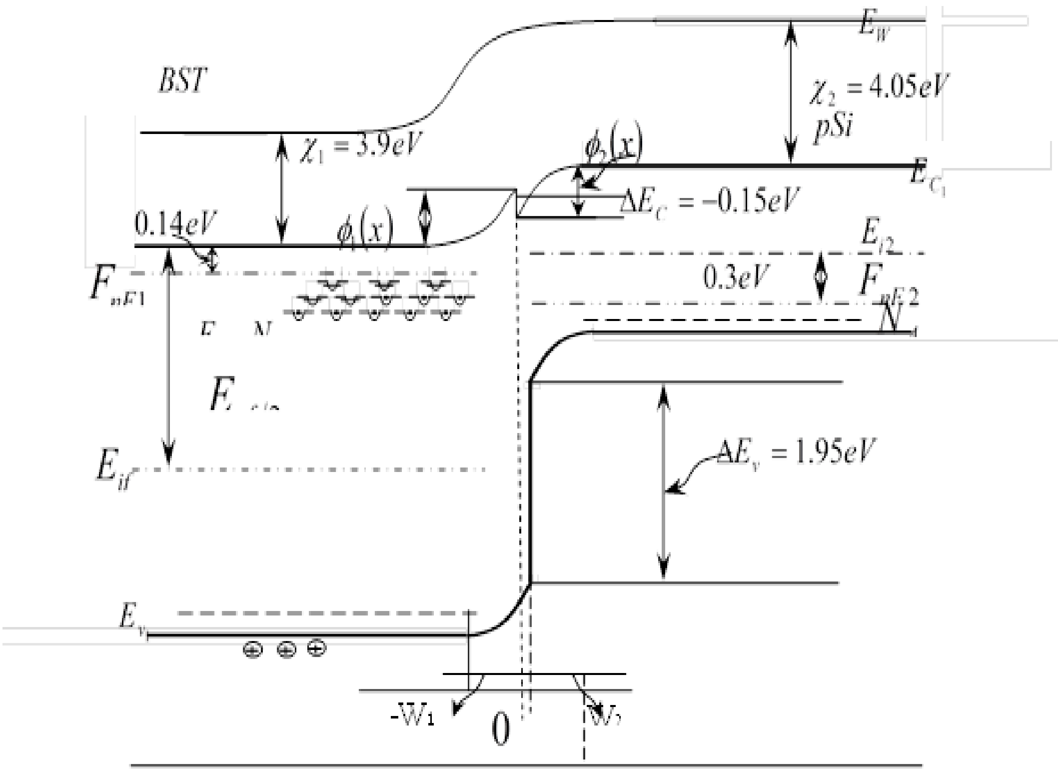

b

Fig.3. The schematic cross-section - (a) and energy band diagram - (b) of the BST/p-Si heterojunction

The energy band diagram (Fig. 3b) corresponds to following other parameters: the band gap of BST and Si are $3.2eV$ and $1.1eV$, respectively, $p-Si$ with a resistivity of $\rho \approx 7\Omega cm$ corresponds to an acceptor concentration of $N_A \approx 2 \cdot 10^{15} cm^{-3}$, concentration of oxygen vacancies $N_t \approx 10^{18} cm^{-3}$ and Fermi quasi level located at $0.31eV$ below from the midgap (intrinsic Fermi level E_{i2}), Fermi-quasi level for electrons in BST is evaluated as $\approx 0.14eV$ below the conduction band E_{cl} and thus the work function for BST becomes $\approx 4.04eV$, the work function of $p-Si$ becomes $\approx 4.91eV$. For the meanings of the other symbols and physical quantities in Fig.3 see [21, 22].

The electrical equivalent circuit of heterojunction structure, neglecting the metal (Ag)-BST Schottky contact depletion layer or diffusion capacitance (depending on polarity of applied voltage) and depletion layer resistance can be presented as it is shown in Fig. 4. In Fig.4, C_f is the BST film conditioned capacitance, $C_h(V)$ is the heterojunction space-charge depletion layer capacitance, R_f is the ferroelectric film resistance, R_h is the heterojunction depletion layer resistance, R_p is the parasitic series resistance resulted from resistance of substrate, resistance of the connected cable, resistance of the pond padswhich can be neglected in compare with the R_f, R_h and C_p is associated with all parasitic capacitances, including stray capacitances of the structure, electrical cables and input capacitances of the measuring system.

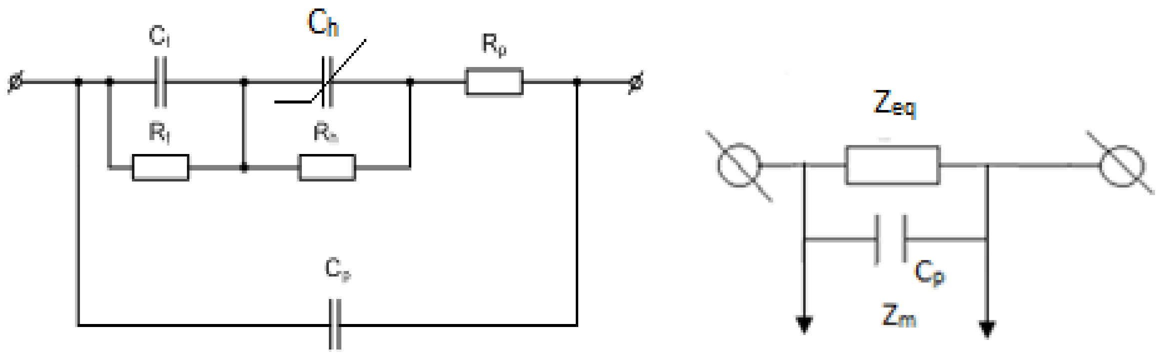

Fig.4. Equivalent circuit of heterojunction structure

Impedance of the considered equivalent circuit (Z_{eq}) is given with the following expressions:

$$Z_{eq} = \frac{1}{1/R_{eq} + (j\omega C_{eq})},$$

$$Z_{eq} = \frac{R_f}{1+(j\omega R_f C_f)} + \frac{R_h}{1+(j\omega R_h C_h)} + R_p = R_{eq} + \frac{1}{j\omega}\left(\frac{1/C_f}{1+1/(\omega R_f C_f)^2} + \frac{1/C_h}{1+1/(\omega R_h C_h)^2}\right), \quad (1)$$

where ω is the angular frequency ($\omega = 2\pi f$),

$$C_{eq} = \left(\frac{1/C_f}{1 + 1/(\omega R_f C_f)^2} + \frac{1/C_h}{1 + 1/(\omega R_h C_h)^2} \right)^{-1}, \quad R_{eq} = \frac{R_f}{1 + (\omega R_f C_f)^2} + \frac{R_h}{1 + (\omega R_h C_h)^2} + R_p \quad (2)$$

Therefore, the measured impedance in air will be given by:

$$Z_m = \frac{1}{1/Z_{eq} + (j\omega C_p)}.$$

In air for all examined frequencies region R_{eq} is high and

$$Z_{eq} \approx \frac{1}{j\omega C_{eq}}.$$

Then the measured impedance will be

$$Z_m(j\omega) \approx \frac{1}{j\omega(C_{eq} + C_p)}, \qquad |Z_m| = \frac{1}{\omega(C_{eq} + C_p)}.$$

Assuming that $C_f \gg C_h(V), R_f \gg R_h(V),$ from the expression (2) one can obtain $C_{eq} \approx C_h(V)$. For example, if estimate the C_f as $C_f \approx \frac{\varepsilon_0 \varepsilon(0) S}{d}$, where ε_0 is the free space dielectric constant $(8.85 \cdot 10^{-12} F/m)$, $\varepsilon(0)$ is the ferroelectric dielectric permittivity at zero field ($\varepsilon(0) \geq 100$, [4,5,8,9]), S is the surface area of BST $(\approx 1cm^2)$, d is the thickness of the ferroelectric thin film $(d \approx 100nm)$ for the C_f we obtain: $C_f \approx 885\,nF$, meantime's, as it shown in [21,22], the $p-Si/Ba_{0.25}Sr_{0.75}TiO_3$ heterojunction space-charge depletion layer capacitance for above mentioned parameters don't exceed $10nF$.

Therefore, it is real assumed that $C_f \gg C_h(V)$ and the Bode plot curves of the structure in air mostly affected by the heterojunction space-charge depletion layer capacitance $C_h(V)$, which is voltage polarity and magnitude dependent.

On the other hand as it is shown in [21,22] were taken into account the nonlinearity of ferroelectric film dielectric permittivity on applied field, E,

$$\varepsilon_f(E) = \frac{\varepsilon_0 \varepsilon(0)}{(1 + AE^2)},$$

where A is constant (for example, for $SrTiO_3$ $A \cong 0.45 \cdot 10^{-11} cm^2/V^2$) [4,5,9,10], as well as taken into account the existence of the high concentration of oxygen vacancies, N_t, in ferroelectric $p-Si$ interfaced layer which in turn is "endowed" ferroelectric to n-type semiconductor properties, $C_h(V)$ can be expressed as [22]:

$$C_h(V) = \frac{\varepsilon_{eff}\left(qN^*\right)^{1/2}}{\sqrt{2(\Phi_{B0} - V_h)\varepsilon_{Si}\varepsilon_0\varepsilon(0)}}, \tag{3}$$

where Φ_{B0} is the heterojunction built-in potential at thermal equilibrium, V_h is the voltage drop in heterojunction, ε_{Si} is the Si dielectric constant,

$$\varepsilon_{eff} \approx \left(\frac{2P_{p0}}{n_{p0}}\right)^{1/2} \frac{\left[n_{p0}p_{p0}N_t\varepsilon_{Si}\varepsilon_0\varepsilon(0)\alpha_1(1+t)\right]}{\left[\alpha_1^2\varepsilon_{Si}N_t^{\,2} + \varepsilon_0\varepsilon(0)N_A^2\right]}, \tag{4}$$

P_{po} and n_{po} are the majority and minority charge carriers in $p-Si$ substrate, respectively, N^* is the effective ions concentration in heterojunction depletion layer, $N^* = \frac{(N_t + N_A)}{N_t N_A}$, where N_A is the acceptor concentration in $p-Si$ substrate. The meanings and physical quantities of the parameters of α_1, t in Eq. 4 are given in [21,22]. As it follows from (3), the value of $C_h(V)$ depends on polarity and magnitude of applied voltage.

3. Conclusions

Thus, in all examined frequency ranges, the Bode plot curves of the $Al - pSi - BST - Ag$ heterojunction structure in air have approximately pure capacitive character. Depending on polarity of applied voltages, the capacitance of structure mostly affected by the heterojunction space charge layer, $C_h(V)$. The parallel shift of Bode plot in air can be explained via the voltage dependence of heterojunction capacitance. For example, when at BST film positive potential is applied in respect to bottom Al contact, this polarity corresponds to forward bias condition of heterojunction (resulting the decrease of the space charge (depletion) layer width and increase of $C_h(V)$ and decrease the capacitive impedance. If at BST film, the negative potential is applied in respect to bottom Al contact, this polarity corresponds to reverse bias condition of heterojunction resulting the increase of the space charge (depletion) layer width, decrease the $C_h(V)$ and increase the capacitive impedance.

Acknowledgments:

This work was supported by the RA MES State Committee of Science in the frame of the research project № *SCS 16YR-2B041.* Authors thanks A. Poghossian for useful discussions and C. Huck from FH Aachen Institute of Nano- and Biotechnologies, University of Applied Sciences (Germany) for performing experiments. The authors gratefully thank J. Schubert from Peter Grünberg Institute (PGI), Forschungszentrum Jülich GmbH, for performing PLD ferroelectric nano-films.

References

[1] E. Barsoukov, J. R. Macdonald, Impedance spectroscopy: Theory, Experiment, and Applications (2nd ed, Wiley-Interscience, Hoboken, NJ, 2005).

[2] A.J. Bard, L.R. Faulkner. Electrochemical Methods: Fundamentals and Applications (2nd ed, John Wiley & Sons Inc. New-York, 2001).

[3] M. Brandt, H. Frenzel, H. Hocmuth et al, J. Vac. Sci. Technol. B27, (2009) 1789.

[4] A.K. Tagantsev, V.O. Sherman, K.F. Astafiev et al, J. Electroceramics 11, (2003)5.
[5] S. Gevorgian. Ferroelectrics in Microwave Devices, Circuits and Systems (Springer-Verlag London, Limited, 2009).
[6] A. Poghossian, M.J. Schöning (In: Encyclopedia of Sensors 9. Eds. C.A. Grimes, E.C. Dickey, M.V. Pishko, 2006,463).
[7] V.V. Buniatyan, M. H. Abouzar, N.W. Martirosyan, et al, Phys. Status Solidi A 207 (2010) 824.
[8] D. Damjanovic, P. Muralt, and N. Setter. Ferroelectric sensors, IEEE Sensors Journal, 1 (2001) 191.
[9] P.Muralt, J. Micromechan. Microeng.10(2000)136.
[10] Z. Ling, C. Leach, R. Fzeer, J. European Ceram. Society, 21 (2001) 1977.
[11] B. Lin, V. Giurgiutiu, Z. Juan et al, Proc. SPIE 6529,(2007) 652901.
[12] G.-A. Racine, P. Muralt and M.-A. Dubois, Smart Mater. Stract.7(1998) 404.
[13] F. Amy, A.S. Wan, and A. Kahn, et al, J. Appl. Phys., 6 (2004) 1635.
[14] H.J. Osten, J.P. Liu, and H.J. Mussig, Appl. Phys. Lett., 80 (2002) 297.
[15] C. Jia, J. Chen, J. Guo et al,NanoscaleResarch Letters6, (2011) 316.
[16] L. Hao, Q. Xue, X. Gao et al, Appl. Phys. Lett., 91(2007) 212105.
[17] Z. Luo, J.H. Hao, J. Gao,Appl. Phys. Lett., 91 (2007) 91.062105.
[18] J. Huang, K. Zhao, H. Lu et al, Physica B 373 (2006) 313.
[19] Ch.-l Hu, P. Han, K. Jin et al, J. App. Phys., 103 (2008) 103-053701.
[20] C.Huck, A.Poghossian, M. Schoening et al, Sens. Actuators B: Chemical 198 (2014) 102.
[21] V. Buniatyan, C.Huck, A. Poghossian et al, Armenian Journal of Physics 6 (2013) 177.
[22] V. Buniatyan, C. Huck, A. Poghossian et al, Armenian Journal of Physics 6 (2013) 188.